Geophys. J. Int. (2006) **167,** 445–452 doi: 10.1111/j.1365-246X.2006.03072.x

Surface motion of a fluid planet induced by impacts

Sidao Ni[1] and Thomas J. Ahrens[2]

[1]*School of Earth and Space Sciences, University of Science and Technology of China, Hefei, Anhui,* 230026, *China*
[2]*Seismological Laboratory,* 252-21, *California Inistitute of Technology Pasadena, CA* 91125, *USA. E-mail: tja@caltech.edu*

Accepted 2006 May 15. Received 2006 May 15; in original form 2006 April 21

SUMMARY

In order to approximate the free-surface motion of an Earth-sized planet subjected to a giant impact, we have described the excitation of body and surface waves in a spherical compressible fluid planet without gravity or intrinsic material attenuation for a buried explosion source. Using the mode summation method, we obtained an analytical solution for the surface motion of the fluid planet in terms of an infinite series involving the products of spherical Bessel functions and Legendre polynomials. We established a closed form expression for the mode summation excitation coefficient for a spherical buried explosion source, and then calculated the surface motion for different spherical explosion source radii a (for cases of $a/R =$ 0.001 to 0.035, R is the radius of the Earth) We also studied the effect of placing the explosion source at different radii r_0 (for cases of $r_0/R = 0.90$ to 0.96) from the centre of the planet. The amplitude of the quasi-surface waves depends substantially on a/R, and slightly on r_0/R. For example, in our base-line case, $a/R = 0.03$, $r_0/R = 0.96$, the free-surface velocity above the source is $0.26c$, whereas antipodal to the source, the peak free surface velocity is $0.19c$. Here c is the acoustic velocity of the fluid planet. These results can then be applied to studies of atmosphere erosion via blow-off caused by asteroid impacts.

Key words: atmosphere, blow-off, giant impact, surface waves.

1 INTRODUCTION

During the early stage of planetary evolution, as a planet grows via impact accretion, the planetesimals which impact upon it increase in mass with time. It is becoming accepted that the Moon could have formed from material ejected from a giant collision on the Earth of a Mar-sized object (Hartmann *et al.* 1986). Ahrens *et al.* (1989) and Ahrens (1993) proposed that such impacts would induce substantial ground motions, and the upper portion of the primordial atmosphere would be accelerated by the ground motion to particle velocities greater than the escape velocity and thus becomes permanently lost to the planet. We recognize that planetary impact is a complex process in which the amplitude of the shock wave caused by the impact decays both via irreversible energy deposition in the vicinity of the impact site and the usual 3-D spherical divergence of spherical wave from a point source. Therefore, we expect that the amplitude of the ground motion induced by P wave would be quite low for sites very far removed from the impact. After comparing this problem with ground motion caused by earthquakes, Ahrens *et al.* (1989) and Ahrens (1993) suggested that a surface wave-like ground motion with a larger amplitude than the direct P wave would be more effective in driving distant ground motions and hence producing atmosphere erosion by the mechanism of particle acceleration with increasing altitude (Zel'dovich & Raizer 1967, p. 859–863). Surface waves caused by shallow earthquakes are generated by the interaction between P and S waves for a solid planet. When a planet is impacted by a giant impactor, we assume that the resulting motion can be approximately described by considering only an acoustic fluid-like wave propagating at the bulk velocity. If only a P-wave propagation occurs, the usual surface waves induced by explosion and impacts are not excited. In this paper, we demonstrate that large surface motions are achievable as a result of the interference of multiply reflected P waves in a fluid planet. This approximation can be applied to examine the degree to which giant impacts can erode substantial portions of an atmosphere. The present paper is an expansion of a summary paper (Ni & Ahrens 2005). Further application of these work to atmospheric blow-off upon giant impact is given in Shen *et al.* (2003) and recently was independently formulated by Genda & Abe (2003a,b).

2 THE MODEL AND EQUATIONS

The process of planetary impact is complicated. We have made approximations as outlined below to make this problem manageable. We assume that a surface impact can be simulated with a buried explosion source (Oberbeck 1971; Hughes *et al.* 1977). We assume that there is a spherical zone of high pressure material below the surface of the planet (Fig. 1). We also assume that the intense shock wave and subsequent elastic wave propagate as attenuation-free acoustic waves in a fluid planet (which has no gravity-restoring force). In this case the waves are governed by the simplified fluid

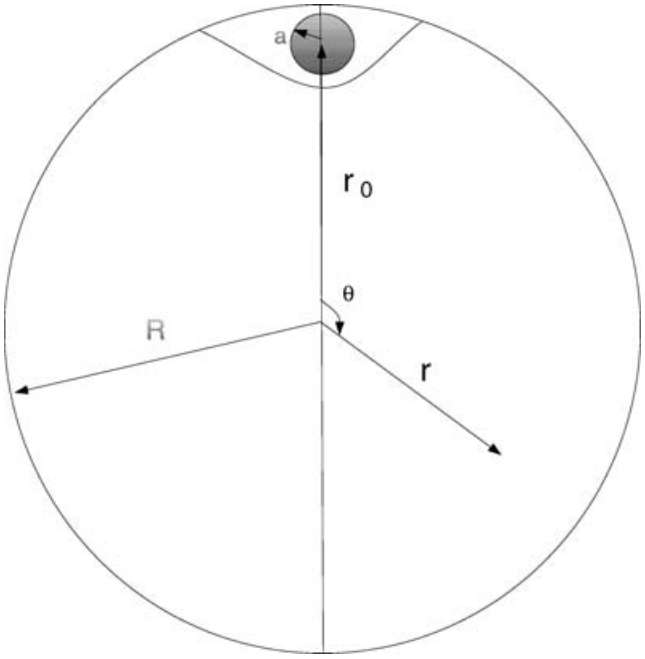

Figure 1. A fluid sphere (radius a at high pressure) is produced upon pressuring an explosive gas-filled cavity, with $P = P_0$ in the source at time $t = 0$.

dynamic equations.

$$\frac{\partial \rho}{\partial t} + \rho_0 \nabla \cdot \vec{u} = 0, \tag{1}$$

$$\rho_0 \frac{\partial \vec{u}}{\partial t} + \nabla P = 0, \tag{2}$$

where ρ_0, u, and P are the density, particle velocity and pressure, respectively. These equations can be further reduced by assuming the isentropic equation of state with a constant acoustic speed $c^2 = (\partial P/\partial \rho)_s$:

$$\partial^2 P/\partial^2 t = c^2 \nabla^2 P. \tag{3}$$

We note that although the density varies with dynamic pressure, this variation, this variation is always around the mean value, p_0, in a planet that lacks gravity. To determine the energy density (per unit mass) deposited in this volume, we first note that this is:

$$E_0 = P_0/(\rho_0 \gamma). \tag{4}$$

Where ρ_0 is density (here taken at 5.51×10^3 kg m^{-3}, the average density of the Earth) and γ equals Gruneissen ratio (here taken as an average $\gamma = 2.0$, typical of Earth materials). Finally we assume for a baseline calculation that

$$P_0 = c^2 \rho_0, \tag{5}$$

where c is the assumed average bulk sound velocity of 10 km s^{-1}, yields $E_0 = 5.0 \times 10^7$ J kg^{-1}. Taking the baseline value of $a = 0.03R$, yields a source energy of 8.1×10^{27} J. This is of same order of that inferred for the impact energy of the K/T extinction bolide (Ahrens & O'keefe 1983).

Initial and boundary conditions are:

$\vec{u}(r, \theta, t)|_{t=0} = 0$; All particles are at rest.

$P(r, \theta, t)|_{r=R} = 0$; Free surface.

$P(r, \theta, t)|_{t \le 0} = P_0$, if the point (r, θ) is in the source zone defined by the spherical region of radius a (coloured region), (*cf.* Fig. 1).

The solution of wave equation (3) is, similar to mode summation in global seismology (Sato *et al.* 1967):

$$P(r, \theta, t) = 2\pi \Sigma_{l,n}^{\infty} A_{ln} j_l \left(\frac{k_{ln} r}{R}\right) P_l(\cos\theta) \cos\left(\frac{k_{ln} c t}{R}\right). \tag{6}$$

The radial particle velocity is; from eq. (2):

$$u_r(r, \theta, t) = 2\pi \Sigma_{l,n}^{\infty} A_{ln} j_l' \left(\frac{k_{ln} r}{R}\right) P_l(\cos\theta) \sin\left(\frac{k_{ln} c t}{R}\right), \tag{7}$$

where $j_l(x)$ is the lth spherical Bessel function (Watson 1922) which is defined as

$$j_l(x) = (\pi/2x) J_{l+1/2}(x)$$

and $J_v(x)$ is the Bessel function.

$j'_l(x)$ is the derivative of $j_l(x)$.

$P_l(x)$ is the ordinary Legendre polynomial. k_{ln} is nth zero of $j_l(x)$, and is usually called the wavenumber.

A_{ln} is the excitation coefficient, and can be calculated from the integral over the source zone.

$$A_{ln} = (2l+1) \frac{\int_0^R \int_0^\pi j_l(k_{ln} r) P_l(cos\theta) P(r, \theta, t = 0) sin(\theta) r^2 \, dr \, d\theta}{k_{ln} j_{l+1}^2(k_{ln})}$$

For the special case of a spherical source with uniform pressure, A_{ln} has the form

$$A_{ln} = 4(2l+1) P_0 \left(\frac{a}{R}\right)^2 j_1\left(\frac{k_{ln} a}{R}\right) j_l\left(\frac{k_{ln} r_0}{R}\right) \Big/ \left(k_{ln} j_{l+1}^2(k_{ln})\right). \tag{8}$$

This result comes from the fact that:

For any point at (r, θ), with r in the range of $r_0 - a < r < r_0 + a$ and for any $0 < \theta < \theta_0$, $\cos(\theta_0) = \frac{r_0^2 + r^2 - a^2}{2 r r_0}$, the pressure $P(r, \theta)$ has a value of P_0. . thus

$$\begin{aligned}
&\int_0^R \int_0^\pi j_l(k_{ln} r) P_l(\cos\theta) P(r, \theta, t = 0) \sin(\theta) r^2 \, dr \, d\theta \\
&= P_0 \int_{r_0 - a}^{r_0 + a} j_l(k_{ln} r) r^2 \int_{\theta_0}^{-\theta_0} P_l(\cos\theta) \, d\cos(\theta) \, dr \\
&= 2P_0 \int_{r_0 - a}^{r_0 + a} j_l(k_{ln} r) r^2 \int_{\cos(\theta_0)}^{1} P_l(x) \, dx \, dr \\
&= 2P_0 \int_{r_0 - a}^{r_0 + a} j_l(k_{ln} r) r^2 \int_{\frac{r_0^2 + r^2 - a^2}{2 r r_0}}^{1} P_l(x) \, dx \, dr \\
&= 2P_0 \frac{a^2}{k_{ln}} j_1(k_{ln} a) j_n(k_{ln} a)
\end{aligned}$$

The last step is based on Theorem 1 in the appendix.

Utilizing the recurrence relation for spherical Bessel functions $j_n'(x) = j_{n+1}(x) + \frac{n}{x} j_n(x)$ and $j_n(k_{ln}) = 0$, we obtained a solution that is simplified for radial velocity at the free surface:

$$\begin{aligned}
&u_r(r = R, \theta, t) = 4\pi \left(\frac{a}{R}\right)^2 \frac{P_0}{\rho c} \\
&\Sigma_{l,n}^{\infty} (2l+1) j_1\left(\frac{k_{ln} a}{R}\right) \frac{j_l\left(\frac{k_{ln} r_0}{R}\right)}{k_{ln} j_{l+1}(k_{ln})} P_l(\cos\theta) \sin\left(\frac{k_{ln} t c}{R}\right)
\end{aligned} \tag{9}$$

As for $u_\theta(r = R, \theta, t)$, the tangential component of the particle velocity on the free surface, it is always zero. This is because $\frac{\partial u_\theta}{\partial t} = \frac{1}{\rho} \frac{\partial P}{\partial \theta}$ (from eq. 2, taking only the tangential component). Given the free surface boundary condition, P is zero on the free surface ($r = R$), thus its tangential gradient $\frac{\partial P}{\partial \theta}|_{r=R}$ is also zero which leads to zero tangential acceleration $\frac{\partial u_\theta}{\partial t}$. Because the initial velocity on the free surface is zero, zero tangential acceleration leads to $u_\theta(r = R, \theta, t) = 0$ for any $t \ge 0$.

3 IMPROVING THE BACKWARD RECURRENCE ALGORITHM OF COMPUTING SPHERICAL BESSEL FUNCTION

Several good numerical approximation methods have been reported for obtaining asymptotic expansions of the spherical Bessel function $j_n(x)$ for very large value of the argument x. Previously the backward recurrence algorithm was used to calculate $j_n(x)$ because of inherent accuracy and machine utilization (Arfken 1995, eqs 11.167 and 11.161). The backward recurrence relation is

$$j_{n-1}(x) = \frac{2n+1}{x} j_n(x) - j_{n+1}(x). \tag{10}$$

Zhang & Jin (1996) use this relation in their Fortran code to calculate $j_n(x)$. The algorithm chooses a large enough number N ($N >> n$) and assumes $j_{N+1}(x) = 0$ for the case of $x < n$. Then by setting $j_n(x)$ to be an arbitrary number, v, eq. (10) is used to calculate the value of $j_{N-1}(x)$, $j_{N-1}(x)$, ..., down to $j_0(x)$. Then the actual value of $v = j_N(x)$ can be obtained using the simple analytical formulae for $j_0(x) = \sin(x)/x$. The backward recurrence algorithm has to be applied when $x < n$, because the forward recurrence (starting from $j_0(x)$ and $j_1(x)$)

$$j_{n+1}(x) = \frac{2n+1}{x} j_n(x) - j_{n-1}(x), \tag{11}$$

is numerically unstable. However, for $x \geq n+1$, forward recurrence is stable. The relevant stability criterion is based on the analysis of the following characteristic equation (obtained by substituting λ for $j_{n+1}(x)$, $j_n(x)$, $j_{n-1}(x)$ in eq. (11)),

$$\lambda^2 = \frac{2n+1}{x}\lambda - 1$$

It can be rewritten as

$$\lambda^2 = A\lambda - 1, \tag{12}$$

where $A = \frac{2n+1}{x}$. Since $x > n$, it is obvious that $A < 2$. The two roots of the above characteristic equation are $\frac{A}{2} \pm i\frac{\sqrt{4-A^2}}{2}$ where i is the unit imaginary number. Therefore, the imaginary parts of the two roots ($A/2$) are <1, and the recurrence based on eq. (12) yields stable result which means that forward recurrence can be used to compute $j_n(x)$ when $x \geq n+1$. Then only n steps of calculation are involved for this forward recurrence scheme. In contrast, the backward recurrence algorithm will involve at least $[x]$ steps of calculation ($[x]$ is the integer part of x). When x is appreciably larger than n, but not large enough to where asymptotic solution become accurate. In general, forward recurrence will converge much faster than backward recurrence approach.

4 NUMERICAL RESULTS

With the analytical solution for radial velocity u_r and the algorithm for calculating high order spherical Bessel functions, we are able to compute ground motion for different values of a and r_0 (the radius of the source zone and the distance of the source zone from the centre of the planet). In Fig. 2, ground motion at different distances (in degrees) from the impact are displayed. The first, P, arrival is indicated by the theoretical P traveltime (solid curve). The later arrivals are multiples such as PP, pPP, PPP, $pPPP$, and they interfere with each other to form a wave train. Near the antipode (distance = 180°), PP (the second arrival) becomes separate, but the multiple reflections of PPP, and $pPPP$, etc interfere with each other and become very

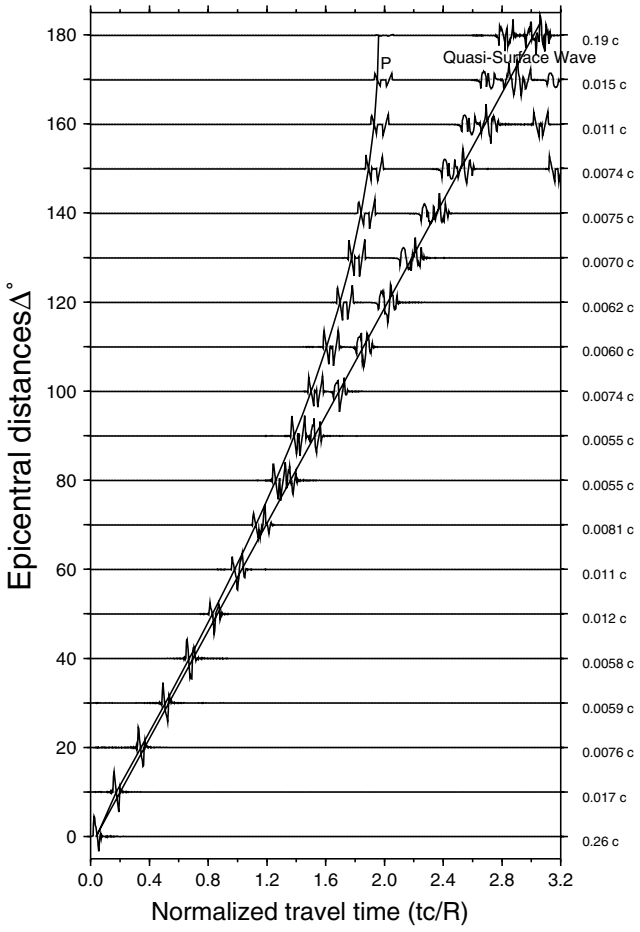

Figure 2. Particle free-surface velocity versus time for different distances for the case of $P_0/\rho c^2 = 1$, $a/R = 0.03$, and $r_0/R = 0.96$. The normalized time is ct/R, where $R = 6371$ km and $c = 10$ km s^{-1}. The solid curve and line denote the geometrical ray arrival of P wave and quasi-surface wave, respectively. Peak values for each particle velocity at the specified distances are given on the right margin. A division on the x-axis represents about 637 s in non-dimensional form. And the maximum particle velocity at the antipode is about 1.9 km s^{-1}.

strong. The direct P wave is almost negligible compared to these waves. At each distance the secondary arrivals appear to propagate with a nearly constant apparent velocity. The almost constant apparent velocity suggests that these interfering waves actually propagate along the surface of the fluid planet. Thus we use the term 'quasi-surface wave' to describe this wave. Buldyrev (1968) analysed the interfering nature of multiple reflections, and found that for 4 or more reflections, ray theory breaks down, and a better approximation must be employed. He called the quasi-surface wave: 'surface wave of interference nature'.

We also investigated the effect of different radii of the source zone. In Fig. 3, we display the quasi-surface wave at the antipode within a time window of $2.9R/c$ and $3.2R/c$. The general feature is that the larger the size of the source zone, the stronger the quasi-surface wave. However, the maximum amplitude does not increase with size monotonically. For example, the maximum amplitude for $a/R = 0.03$ is larger than that for $a/R = 0.035$. This is caused by the interfering nature of the quasi-surface, for $a/R = 0.03$ some arrivals are strengthening each other and produce large amplitudes, while for $a/R = 0.035$ those arrivals show less positive interference effects. This again supports the idea that quasi-surface waves are results of

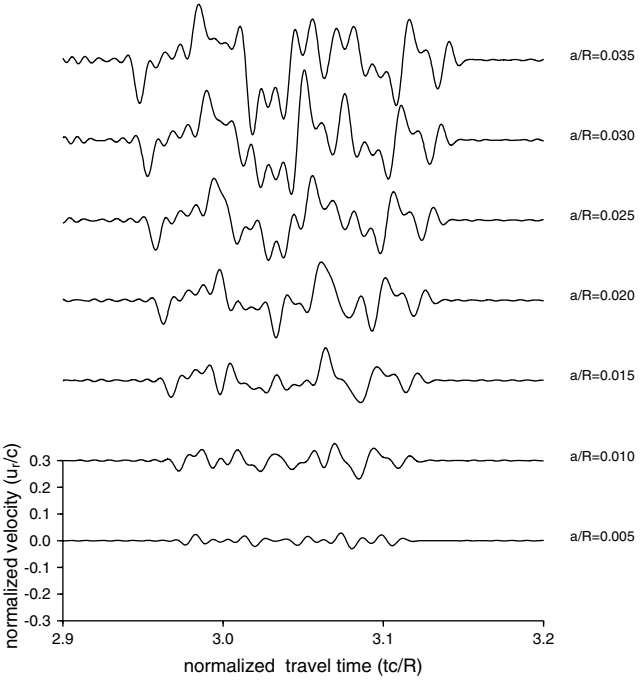

Figure 3. Quasi-surface wave at antipode for different radii of source zone, a, for $r_0/R = 0.96$. The values of radii are indicated at right margin. Generally, larger source zone induces larger quasi-surface wave.

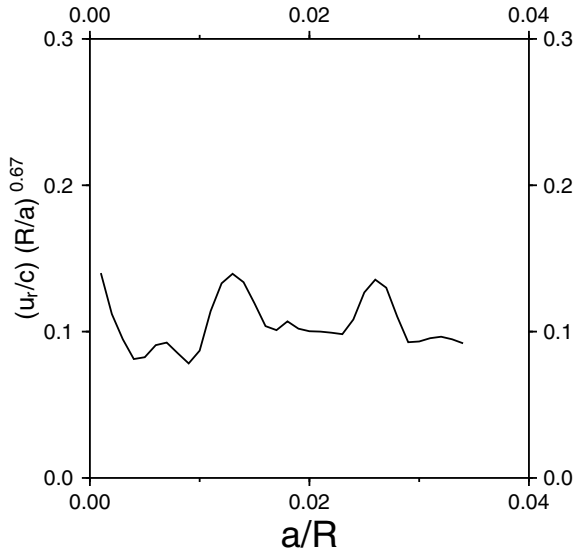

Figure 4. An attempt of modelling the dependence of the peak velocity at antipode on the radius of the source zone for the case of $r_0/R = 0.96$. The vertical axis represents the ratio of $\frac{u_r/c}{(a/R)^{0.67}}$, which is almost constant for different ratio of a/R. The two peaks at $a/R \approx 0.013$ or 0.026 are probably caused by interference effects.

interference. To study the dependence of the peak velocity on the radius of the source, we assume a power law dependence in the form of $u_r \propto a^k$ and then explore different values of k. It appears that for $k \approx 0.67$, the ratio of u_r/a^k is nearly constant for different values of a (Fig. 4). However, there are peaks of velocity at $a/R \approx 0.013$ or 0.026 which are probably caused by constructive interference.

It is also interesting to explore the effect of depth of the source zone because the equivalent depth of a buried explosion appropriate for an impact is not well studied. Ground motions for different depths are displayed in Fig. 5. The source zone is chosen to be small ($a/R = 0.005$) so as to make each reflected wave more impulsive and to facilitate identification of each reflected wave. For very deep source ($r_0/R = 0.90$), only *PPP* and *pPPP* are observed. For $r_0/R = 0.92$, *pPPP* and *pPPPP* appear. However, for $r_0/R > 0.95$, multiple reflections such as *PP*, *PPP* arrive nearly simultaneously and produce complicated waveforms. This is just predicted by Buldyrev's theory that for more than four reflections, ray theory is no longer applicable. It appears that for depths $r_0 > 0.90$, the maximum amplitude does not change much by further varying the source depth, though the duration of quasi-surface wave becomes longer with shallower depth.

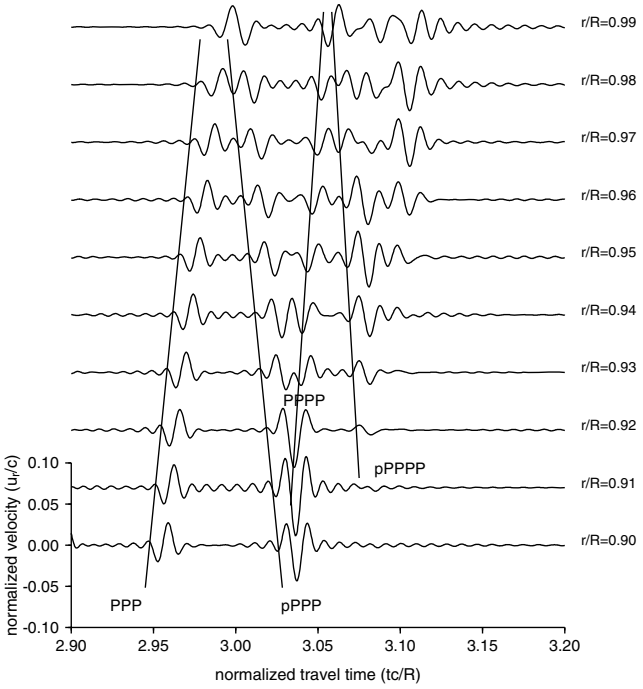

Figure 5. Quasi-surface wave at the antipode for different depths. The size of source zone is ($a/R = 0.005$). For very deep source, multiple reflection *PPP*, *pPPP* can be identified. For shallower depths, *pPPP*, and *pPPPP* can be identified. However, for source shallower than $0.95R$, ray theory is no longer applicable as predicted by Buldyrev (1968).

The effects of a and r_0 on the amplitude of peak velocity can be best revealed in Fig. 6 where contours of peak velocity versus a and r_0 are displayed. Generally, larger a/R yields larger velocity. Especially, for small value of a/R, the contours are nearly vertical lines, indicating that the peak velocity does not depend on r_0. However, for some values of a/R (e.g. ≈ 0.013 or 0.026), the contours are bent towards to the left, suggesting that, even with smaller a/R, the same amplitude of velocity can be achieved.

5 DISCUSSION AND CONCLUSION

We have studied a very idealized situation for planets impacted by Mars-sized asteroids. By assuming that the shock wave propagation can be approximated by an acoustic wave and approximating the impact region as buried spherical pressure source, we are able to derive an analytical solution for the ground motion. Numerical calculation for different sizes and depths of the source zone reveals the interference nature of quasi-surface wave. At the antipode, the quasi-surface is much stronger than the direct shock wave, thus

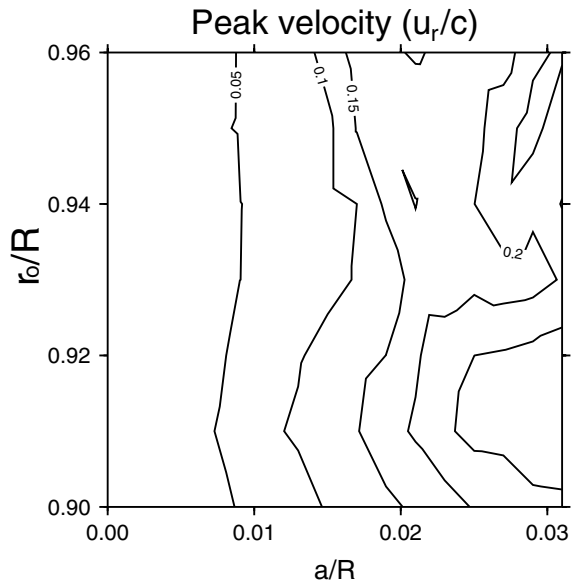

Figure 6. Contours of peak velocity at antipode versus radius of source zone (a/R) and distance of source zone from centre of planet (r_0/R). Note that r_0/R does not strongly affect the peak velocity as contours are almost vertical lines. When a/R is larger (>0.02), complexity of contours occurs suggesting that interference effects are important.

making possible atmosphere erosion by giant impactors. Although the impactor with energy E_0 assumed in this study only excites ground motion up to 2 km s^{-1}, which would not cause much atmospheric loss (Genda and Abe 2004a,b), more energetic impactor will excite stronger ground motion, thus leading to substantial blow-off of atmosphere (the particle velocity of free surface motion is scaled with $\sqrt{(E/E_0)}$, Ahrens *et al.* (2004). We also realize that we have neglected the effect of radial structure of the planet and self gravitation which only moderately affects impact-induced motion (Ni & Ahrens 2004). More refined analysis should be performed for a more realistic simulation of impact processes.

We also proposed a stable and accurate algorithm for calculating spherical Bessel functions for very high orders. We have also found some new identities involving spherical Bessel functions and Legendre polynomials, which are expected to be useful for further studying the ground motion of radially structured planets.

ACKNOWLEDGMENTS

We thank two anonymous reviewers and editor Bruce Buffett whose comments greatly improve the manuscript. Research supported by NASA grant NNG04GI07G, and supported by NSFC grant 40425005. Contribution # 8957, Division of Geological and Planetary Sciences, California Institute of Technology, Pasadena, CA 91125.

REFERENCES

Ahrens, T.J., 1993. Impact erosion of terrestrial planetary atmosphere, *Annu. Rev. Earth. Sci.,* **21,** 525–555.

Ahrens, T.J., O'Keefe, J.D. & Lange, M.A., 1989. Formation of atmosphere during accretion of the terrestrial planets, in *Origin and Evolution of Planetary and Satellite Atmospheres,* pp. 328–385, eds Atreya, S.K., Pollack, J.B. & Mathews, M.S. U. Ariz. Press, Tucson, AZ.

Ahrens, T.J., Shen, A.H. & Ni, S., 2004. Giant Impact Induced Atomospheric Blow-off, *13th APS Topical Conference on Shock-Compression of Condensed Matter,* ed. Furnish, M.D., Amer. Inst. Phys., College Park, Maryland.

Arfken, G., 1995. *Mathematical methods for physicists,* Academic Press, Orlando, pp. 551–559.

Buldyrev, V.S., 1968. Wave propagation near the curved surface of an inhomogeneous body, Spectral theory and problems in diffraction, *Topics in Mathematical Physics,* **Vol. 2,** Consultants Bureau. New York. pp. 115–119.

Chen, G.Q. & Ahrens, T.J., 1997. Erosion of terrestrial planet atmosphere by surface motion after a large impact, *Phys. Earth planet. Inter.,* **100,** 32–47,

Genda, H. & Abe, Y., 2003a. Survival of a protoatmosphere through the stage of Giant impacts: the mechanical aspects. *Icarus,* **164,** 149–162.

Genda, H. & Abe, Y., 2003b. Survival of a protoatmosphere through the stage of Giant impacts (abstract), in *Lunar and Planetary Science, 1623.pdf,* Lunar and Planetary Science Institute, Houston, Texas.

Gradshtein, I. & Ryzhik, I., 1965. *Table of Integrals, Series, and Products,* pp. 233–234 Academic Press, New York.

Hartmann, W.K., Philips, R.J. & Taylor, G.J., 1986. Origin of the Moon, pp., 781, Lunar and Planetary Institute, Houston

Hughes, H.G., App, F.N. & McGetchin, T.R., 1977. Global Seismic effects of basin-forming impacts, *Phys. Earth planet. Inter.,* **15,** 251–263.

Ni, S. & Ahrens, T.J., 2005. Giant impact-induced blow-off of primordial atmosphere, *Geol. Soc. Am., special paper,* 384–25.

Oberbeck, V.R., 1971. Laboratory simulation of impact cratering with high explosives, *J. geophys. Res.,* **76,** 5732–5749.

Sato, Y., Usami, T. & Landisman, M., 1967. Theoretical seismograms of torsional disturbances excited at a focus within a heterogeneous spherical Earth; case of a Guttenberg-Bullen A'earth Model. *Bull. of the Earthquake Res. Inst.,* **45**(3), 601–624.

Shen, A.H., Ahrens, T.J. & Ni, S., 2003. Erosion of planetary atmosphere due to surface wave induced by Giant impact (abstract), *Lunar and Planetary Science,* **XXXIV,** CD 2031.pdf.

Watson G. N., 1922. *A Treatise on the Theory of Bessel Functions,* Cambridge U. Press, Cambridge, UK, pp. 195–261.

Zhang, S. & Jin, J., 1996, *Computation of Special Functions,* John Wiley Press, New York, pp. 100–120.

Zel'dovich, Y.B. & Raizer, Y.P., 1966. *Physics of Shock Waves and High-Temperature Hydrodynamic Phenomena,* Vol. 112. New York, Academic, p. 916.

APPENDIX A: SPHERE INTEGRAL OF SPHERICAL BESSEL FUNCTION AND LEGENDRE POLYNOMIALS

In this paper, the spherical Bessel functions is denoted as $j_n(x)$, and is defined as $j_n(x) = \sqrt{\frac{\pi}{2x}} J_{n+1/2}(x)$ where $J_{n+1/2}(x)$ is the ordinary Bessel function (Arfken 1995, 11.141). The Legendre polynomial is denoted as $P_n(x)$. We found that an integral of the product of spherical Bessel function and Legendre polynomials over a spherical volume can be reduced to a simple closed form, as stated in the following theorem:
Theorem 1.

$$I_n = \int_{r_0-a}^{r_0+a} j_n(\omega r) r^2 \int_f^1 P_n(x)\,dx\,dr = 2\frac{a^2}{\omega} j_1(\omega a) j_n(\omega r_0) \tag{A1}$$

Where $f = \frac{r^2+r_0^2-a^2}{2rr_0}$, $r_0 \geq a \geq 0; n \geq 0$.

To prove the theorem, we introduce another identity of Legendre polynomials.
Lemma 1.

$$r_0^n \frac{\partial}{\partial r_0}\left(r_0^{-n}\int_f^1 P_n(x)\,dx\right) = -r^{-(n+2)}\frac{\partial}{\partial r}\left(r^{n+2}\int_f^1 P_{n+1}(x)\,dx\right), \tag{A2}$$

or

$$r_0^n \frac{\partial}{\partial r_0}\left(r_0^{-n}\frac{P_{n-1}(f)-P_{n+1}(f)}{2n+1}\right) = -r^{-(n+2)}\frac{\partial}{\partial r}\left(r^{n+2}\frac{P_n(f)-P_{n+2}(f)}{2n+3}\right), \tag{A3}$$

where $f = \frac{r^2+r_0^2-a^2}{2rr_0}$, and $n \geq 1$

Proof

When $n \geq 1$, we have (Arfken 1995; eq. 12.23)

$$P'_{n+1}(x) - P'_{n-1}(x) = (2n+1)P_n(x)$$

Thus

$$\int_f^1 P_n(x)\,dx = \frac{P_{n-1}(f)-P_{n+1}(f)}{2n+1}$$

which uses the fact that $P_n(1) = 1$ for all $n \geq 0$

Note that:

$$\frac{\partial f}{\partial r} = \frac{1}{2r_0} - \frac{r2_0 - a2}{2r_0 r} = \frac{1}{r_0} - \frac{f}{r}$$
$$\frac{\partial f}{\partial r_0} = \frac{1}{2r} - \frac{r2 - a2}{2r_0 r} = \frac{1}{r} - \frac{f}{r_0}$$

Then, by expanding the left-hand side (LHS) of (A3) with differentiation by parts, we have

$$\text{LHS (A3)} = r_0^n \frac{-n}{r_0^{n+1}}\frac{P_{n-1}(f)-P_{n+1}(f)}{2n+1} + r_0^n \frac{1}{r_0^n}(-P_n(f))\left(\frac{1}{r}-\frac{f}{r_0}\right)$$
$$= \frac{nP_{n+1}(f) - nP_{n-1}(f) + (2n+1)fP_n(f)}{(2n+1)r_0} - \frac{P_n(f)}{r}$$

With the identity (Arfken 1995; eq. 12.17)

$$(2n+1)xP_n(x) = (n+1)P_{n+1}(x) + nP_{n-1}(x),$$
$$\text{LHS of (A3)} = \frac{P_{n+1}(f)}{r_0} - \frac{P_n(f)}{r} \tag{A4}$$

And the right-hand side:

$$-\text{RHS of (A.3)} = \frac{1}{r^{n+2}}(n+2)r^{n+1}\frac{P_n(f)-P_{n+2}(f)}{2n+3}\frac{r^{n+2}}{r^{n+2}}(-P_{n+1}(f))\left(\frac{1}{r_0}-\frac{f}{r}\right)$$
$$= \frac{(n+2)P_n(f) - (n+2)P_{n+2}(f) + (2n+3)fP_{n+1}(f)}{(2n+3)f} - \frac{P_{n+1}(f)}{r_0}$$

With eq. (4), then

$$\text{RHS (of A3)} = -\left\{\frac{P_n(f)}{r} - \frac{P_{n+1}(f)}{r_0}\right\} = \text{LHS}$$

Lemma 1 proved.

Now, we can prove the theorem (by induction).

Proof of theorem 1.

Note that (Arfken 1995, eqs 11.148, 11.154 and 12.1])

$$j_0(x) = \frac{\sin(x)}{x}$$
$$j_1(x) = \frac{\sin(x) - x\cos(x)}{x^2}$$
$$P_0(x) = 1$$

When $n = 0$

$$I_0 = \int_{r_0-a}^{r_0+a} \frac{\sin(\omega r)}{\omega r} r 2\left(1 - \frac{r^2 + r_0^2 - a^2}{2rr_0}\right) dr$$
$$= \frac{1}{2\omega r_0}\int_{r_0-a}^{r_0+a} \sin(a^2 - (r - r_0)^2)\, dr$$

(With change of variable $y = r - r_0$)

$$= \frac{1}{2\omega r_0}\int_{-a}^{a} \sin(\omega(r_0 + y))(a^2 - y^2)\, dy$$

Note that

$$\sin\omega(r_0 + y) = \sin\omega r_0 \cos\omega y + \cos\omega r_0 \sin\omega y$$

and that $\sin(x)$ is an odd function, and $(a^2 - x^2)$ is an even function

$$\int_{-a}^{a} \sin\omega y(a^2 - y^2)\, dy = 0$$
$$\int_{-a}^{a} \cos\omega y(a^2 - y^2)\, dy = \frac{4}{\omega^3}\frac{\sin\omega a - \omega a\cos\omega a}{(\omega a)2}(\omega a)^2$$
$$= \frac{4}{\omega} j_1(\omega a)(a)^2$$

Hence

$$I_0 = 2\frac{a^2}{\omega} j_1(\omega)\frac{\sin\omega r_0}{\omega r_0} = 2\frac{a^2}{\omega} j_1(\omega a) j_0(\omega r_0)$$

Assume that for any $k \geq 1$,

$$I_k = 2\frac{a^2}{\omega} j_1(\omega a) j_k(\omega r_0). \tag{A5}$$

With the indentity

$$\frac{d}{dx}\left(x^{n+1} j_n(x)\right) = x^{n+1} j_{n-1}(x), \tag{A6}$$

$$\frac{d}{dx}\left(x^{-n} j_n(x)\right) = -x^{-n} j_{n+1}(x). \tag{A7}$$

Then we have:

$$r_0^k \frac{\partial}{\partial r_0}\left(r_0^{-k} I_k\right)$$
$$= r_0^k \frac{\partial}{\partial r_0}\left(r_0^{-k} 2\frac{a^2}{\omega} j_1(\omega a) j_k(\omega r_0)\right)$$
$$= -2\omega\frac{a^2}{\omega} j_1(\omega a) j_{k+1}(\omega r_0) \tag{A8}$$

However, another way of evaluating the LHS of eq. (A8) is

$$r_0^k \frac{\partial}{\partial r_0}\left(r_0^{-k} I_k\right) = r_0^k \frac{\partial}{\partial r_0}\left\{\int_{r_0-a}^{r_0+a} j_k(\omega r) r^2 r_0^k \int_f^1 P_n(x)\,dx\,dr\right\}$$
$$= r_0^k\left[j_k(\omega r) r^2 r_0^k \int_f^1 P_n(x)\,dx\right]_{r_0-a}^{r_0+a} + \int_{r_0-a}^{r_0+a} j_k(\omega r) r^2 r_0^k \frac{\partial}{\partial r_0}\left(r_0^{-k}\int_f^1 P_n(x)\,dx\right) dr$$

Note that $f = 1$ at $r = r_0 \pm a$, thus the first term of the last line is zero.

The second term should be (using Lemma 1 and integrating by parts)

$$\int_{r_0-a}^{r_0+a} j_k(\omega r) r 2(-1) r^{-(k+2)} \frac{\partial}{\partial r}\left(r^{k+2}\int_f^1 P_{n+1}(x)\,dx\right) dr$$
$$= -\left[j_k(\omega r) r^2 r^{-(k+2)}(r^{k+}) \int_f^1 P_{n+1}(x)\,dx\right]_{r_0-a}^{r_0+a}$$
$$+ \int_{r_0-a}^{r_0+a} r^{k+2}\int_f^1 P_{k+1}(x)\,dx \frac{\partial}{\partial r}(r^{-k} j_k(\omega r))\,dr$$

(the first term is 0 because $f = 1$ at $r = r_0 \pm a$)

(with eq. 7)

$$= \int_{r_0-a}^{r_0+a} r^{k+2}\int_f^1 P_{k+1}(x)\,dx\left(-\omega r^{-k} j_{n+1}(\omega r)\right) dr$$
$$= \int_{r_0-a}^{r_0+a}\int_f^1 P_{k+1}(x)\,dx(-\omega r^2 j_{n+1}(\omega r))\,dr$$
$$= -\omega I_{k+1}$$

Thus,

$$I_{k+1} = 2\frac{a^2}{\omega} j_1(\omega a) j_{k+1}(\omega r_0)$$

Then, according the principle of mathematical induction, eq. (A1) must be true for all n.